

EUROFEL-Report-2007-DS4-092

EUROPEAN FEL Design Study



Deliverable N°: D 4.4
Deliverable Title: First stage of harmonic generation - Summary
Task: DS-4
Authors: see next page
Contract N°: 011935

**Project funded by the European Community
under the “Structuring the European Research Area” Specific Programme
Research Infrastructures action**

D 4.4 Report - First stage of harmonic generation

Mathias Brandin, Nino Cutic, Filip Lindau, Sara Thorin, Sverker Werin; MAX-lab Lund University, Lund, Sweden

J. Bahrtdt, H.-J. Bäcker, W. Frentrup, A. Gaupp, K. Goldammer, K. Holldack, A. Meseck, Dmytro Pugachov^{*)}, M. Scheer; BESSY, Berlin, Germany

J. Kuhnenn; Fraunhofer INT, Euskirchen, Germany

^{*)} also at MAX-lab

Introduction

This is the final report summarising the work in *DS 4.1 First stage of harmonic generation*.

In collaboration between the synchrotron radiation laboratory MAX-lab in Lund, Sweden and BESSY in Berlin, Germany, a test facility for a seeded Harmonic Generation (HG)-FEL [1] has been built at the MAX-laboratory in Lund. The test facility uses the existing MAX injector and provides an opportunity for investigating the design and function of various aspects of the FEL and also for testing simulation codes and scripts. The project also shows how a synchrotron radiation facility can be upgraded and used for FEL research.

The MAX injector [2] with its capabilities of up to 500 MeV electrons has been equipped with an optical klystron (OK), consisting of two undulators and a chicane, and a gun and seed laser system plus a complete beamline for the test-FEL (see fig 1).

Additionally simulations of the facility have been performed by BESSY and MAX-lab jointly. A radiation dose measuring system has also been installed and tested. First initial tests of subsystems of the set-up have been performed and the production of coherent photons is planned for the near future.

1 Overall description of the project

The FEL test facility collaboration is structured such that MAX-lab provides the high quality electron beam together with a seed laser for the experiment and BESSY will construct and install the FEL undulators. Electron and photon beam diagnostics as well as commissioning and operation of the FEL will be managed in close collaboration.

The injector consists of two 5.2 m long linac structures each providing for a beam energy of up to 125 MeV. When the electrons have passed both linacs they will be bent into a recirculator, turning them around 360 degrees and passing them through the linacs one more time. This gives a total beam energy of 400-500 MeV. An achromatic dogleg is commonly used as a translating stage in beam transports and in this setup both compresses the electron bunches and elevates the beam from the cellar to ground level. The FEL undulators [3] are placed inside the MAX II ring, approximately 40 m from the injector (fig. 2). Just before the first undulator, the electrons will do a 20 mm translation so that a seed laser beam can be inserted. The FEL section comprises of one planar and one APPLE II type undulator and an intermediate magnetic chicane. This will make up a one stage HG FEL, seeded with a Ti:Sapphire laser at 266 nm. A



Fig 1. The beamline at MAX-lab with the two undulators of the optical klystron and the chicane in the middle. In the background the laser hutch for the seed laser system.

complete commercial laser system has been purchased from Thales SA and has been installed at MAX-lab. This laser provides not only a 500 fs seeding pulse but gives also a fully synchronized 10 ps pulses to be used for the photo injector.

2 Start to end simulations

The creation of short, intense and coherent radiation pulses with the development of Free Electron Lasers is an important step for future light sources. The FEL interaction, though, requires a high quality electron beam with high peak current, low energy spread and low emittance and therefore a high performance source.

The test-FEL performance has been investigated by start-to-end simulations. These simulations are exemplified by the work done on the stage two of the set-up which utilises an improved RF-gun system with lower emittance and higher bunch charges.

266 nm laser pulse and the undulators are tuned to give radiation at either the third or fifth harmonic which corresponds to 88 and 53 nm.

Simulating the different parts of the machine using different codes lets us do the right approximations for each part and conversion of the output using Matlab makes it possible to automatically run a simulation through several codes. By doing start-to-end calculations [4] from the gun through the recirculator and transport to the end of the optical klystron we will get an idea of the performance of the FEL and can optimize the whole setup on the final result, the radiation. It will also give us a chance to compare the simulation results with experiments.

The Gun

In order to produce a transversely and energetically collimated electron beam, the electrons are generated in a low emittance photo cathode gun. The beam dynamics in the gun is simulated with the

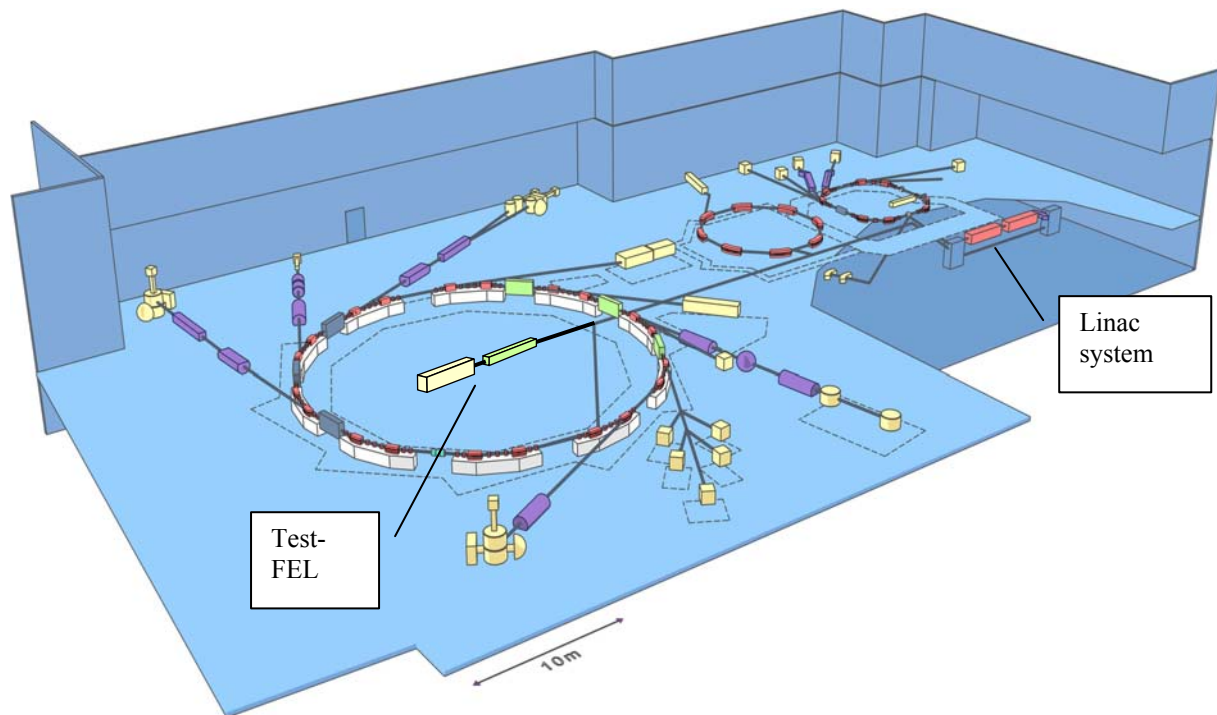


Fig 2. MAX-lab and the location of the test-FEL.

By using an off crest RF phase in the MAX-lab linac and adjusting the magnetic optics in the translating dogleg in the transport line, longitudinal compression of the electron bunch can be achieved. Since the compression is done after total acceleration the electron bunches will have a relatively high energy spread. The RF phase and compression therefore have to be optimized with final energy spread as a more important factor than high current in order to get maximum light output power. The FEL interaction is seeded with a 500 fs,

code ASTRA [5] which takes into account space charge effects. After the gun the electron beam is bent approximately $10 \mu\text{rad}$ to go centered through the linac. This bend is simulated in ELEGANT [6] where a conversion of the output file between ASTRA and ELEGANT is done in Matlab. The particle file is then converted back to ASTRA input and run through the first linac in the MAX-injector. The beam parameters at the exit from the gun can be seen in table 1 and figure 3.

Table 1: Beam parameters after the gun

Energy	8	MeV
Energy spread	3	%
Normalized emittance	3	mm mrad
Pulse length(fwhm)	11	ps
Peak current	45	A
Charge	0.5	nC

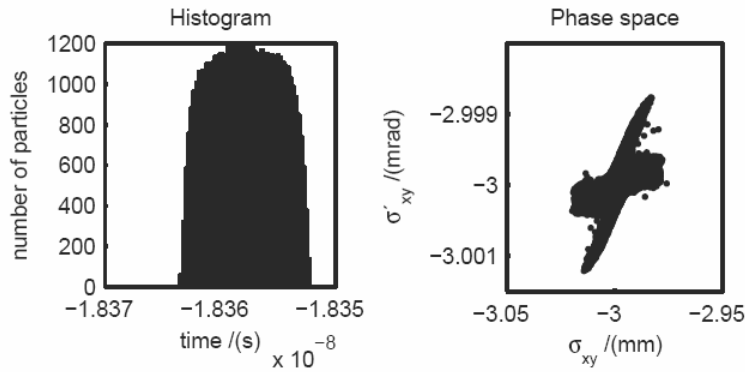


Fig. 3. Time structure and transversal phase space of the electron beam after the gun.

bending blocks, dipoles, quadrupoles and sextupole magnets are used. The sextupoles are used to correct slightly for second order effects that appear from the sinusoidal shape of the accelerating field. These sextupoles are however already integrated into some of the quadrupoles and can not be tuned separately and completely compensate for the second order effects. The optics in the recirculator is such that the energy of the beam on the second turn through the linac has to be twice that of the first turn for the electrons to enter the transport line properly.

Transport

The transport from the injector to the undulator section is about 40 m and includes a vertical lift of the beam from the cellar to the ground floor, see figure 5. This lift is done with an achromatic dogleg consisting of two 15 degree bends with 5 quadrupoles in between. The middle quadrupole is used to

control the beta-function while the two outer ones are used to close dispersion after the second bend. To avoid space charge effects in the centre of the

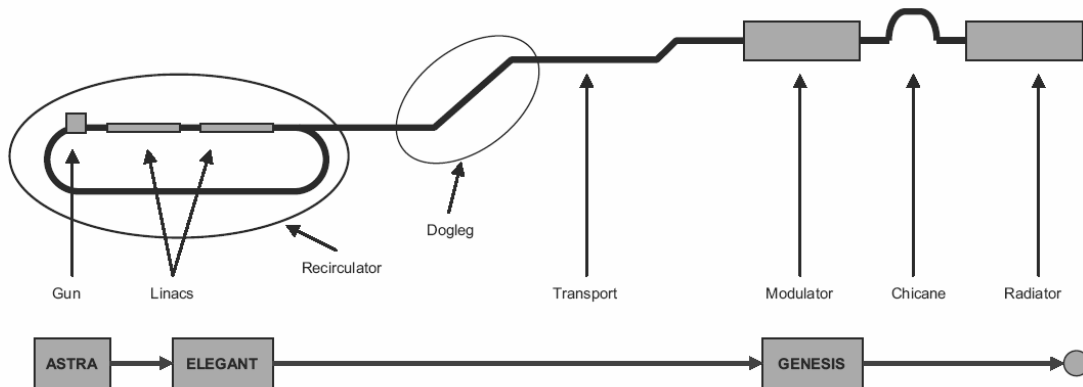


Fig 4. Schematic view of the FEL setup and simulations.

The Recirculator

As mentioned earlier a recirculating system is used at MAX-lab to accelerate the electrons to their full energy (see fig. 4). To make the two 180 deg

dogleg, where the beta function can hit a very low minimum, the two quads on either side of the middle are used for modification of the beta function. The dogleg also introduces an $R56$ suitable for compressing the electron bunch. Near the end of the transport section there is a half chicane used to align the seed laser pulse with the electron beam. This bend is done upwards, which is in the bending plane of the electrons in the undulator, and gives a small dispersion to the beam in the y direction.

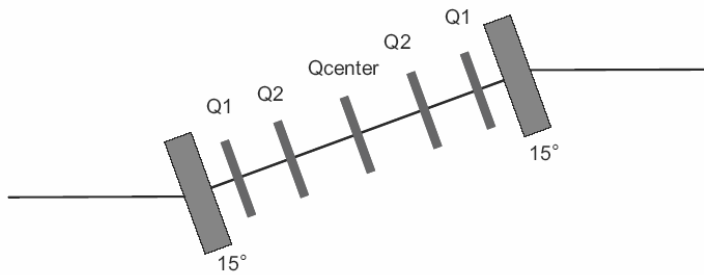


Fig. 3. Drawing of the translating dogleg where the bunch compression is done.

It is however small enough to not influence the beam size noticeably. The optics in the transport is set to give a beam waist inside the first FEL undulator. The transversal rms size of the beam at the minimum is in the order of $250 \mu\text{m}$, which corresponds to the size of the seed laser at this point. The resultant beta and dispersion functions after optimization can be seen in figure 6.

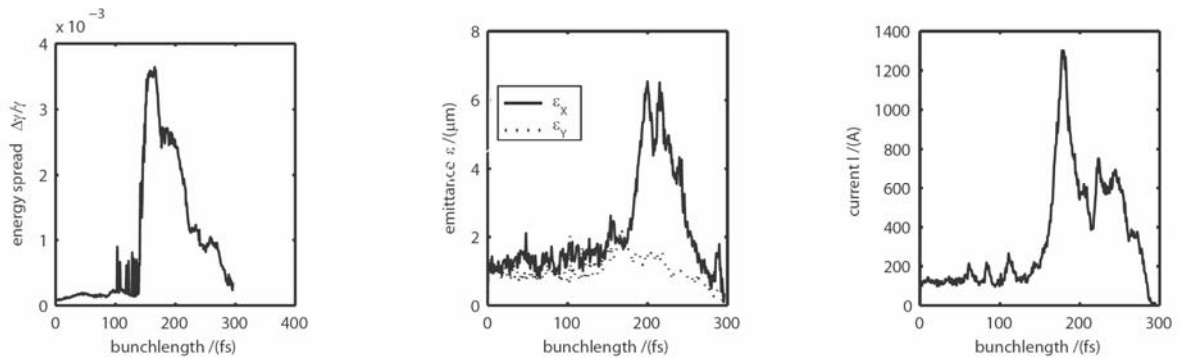


Fig. 4. Sliced energy spread, emittance and current just before the undulator section.

Bunch Compression
 Since a high peak current is important for FEL efficiency, the electron bunches have to be compressed after the gun. In this already existing machine there is no room to install a compressor chicane, but the dogleg in the transport can be used as a bunch compressor. The method is similar to the common bunch compression schemes in linear accelerators[8]: the electric field in the linac is given such a phase that an energy chirp is induced in the electron pulses. Through the quadrupoles and dipoles in the transport dogleg, this chirp can then be rotated time wise to result in a very short pulse. Optimizations, matching and calculations of R_{56} , dispersion and twiss parameters were made partially in DIMAD[9] and partially by hand through a GUI written in MATLAB that lets you change the optics along the machine and check the corresponding twiss parameters and R_{56} .

After optimizing the dogleg for both optics and compression it gives an R_{56} of 5.5 cm which means

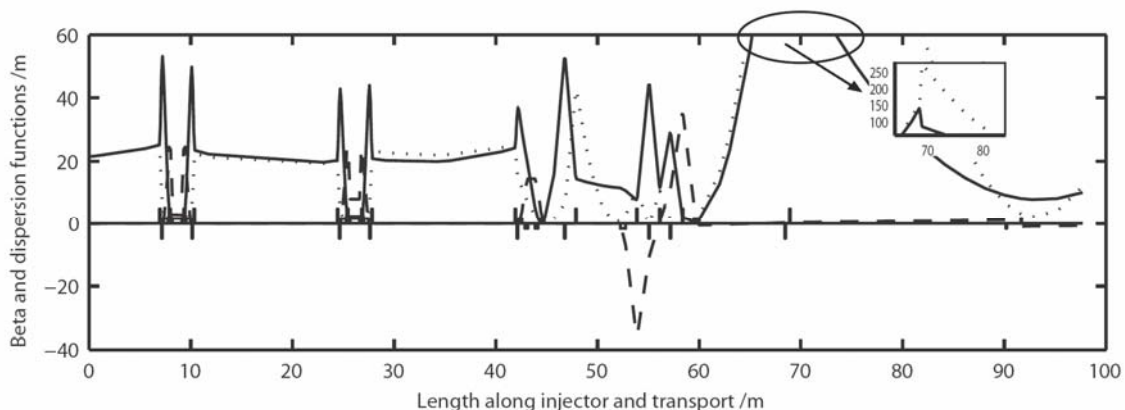


Fig. 5. Twiss parameters

that an accelerating phase of 30 deg would be ideal and give the best compression. However, in the recirculating system in the MAX-lab injector the electrons have to have twice the energy on the second pass though the linacs compared to the first

pass in order to be extracted into the transport line. This gives the condition that the accelerating phase has to be the same in both passes through the linacs and taking dispersion, beam size and energy spread into account a much lower accelerating phase had to be used. After investigating a series of cases a phase of 8 degrees was found to be optimal. This optimization was made to get the highest output laser power on the third harmonic. Approximately 20% of the bunch charge can be confined within a 300 fs (90 μm) long part of the bunch with a mean current of 300 A. The peak current goes up to 1.3 kA in the main peak but in this region the energy spread is quite high ($\Delta\gamma/\gamma = 0.25\%$). There is also a few peaks with lower current and lower energy spread of about 700 A and $\Delta\gamma/\gamma = 0.09\%$. The reason for the relatively high energy spread is that all compression is done after acceleration due to the structure of the injector facility. Table 2 gives the beam parameters and figure 7 show a slice analysis of the beam at the exit of the beam transport.

The demands on the electron beam before entering the undulators are low sliced emittance, low sliced energy spread, high peak current, and matched transverse size. The output from ELEGANT is converted using Matlab into a format compatible with GENESIS 1.3 [9] where the FEL simulations [10] are done.

Table 2. Beam parameters of the compressed electron bunch just before entering the FEL undulators

<i>First peak (Second peak)</i>		400	MeV				
Energy		0.25%	(0.09%)				
Energy spread		4	mm	mmrad	(4	mm	mmrad)
Normalised emittance		30	fs	(30	fs)		
Pulse length(fwhm)		1.3	kA	(700	A)		
Peak current		0.04	nC	(0.02	nC)		
Charge							

FEL Undulator section

The FEL section comprises of two undulators and an intermediate magnetic chicane. In the first undulator, called modulator, the electron beam co propagates with a strong seed laser of 266 nm wavelength and is modulated in energy. The particles then pass through the magnetic chicane which serves as a dispersive element. It consists of four dipole magnets and introduces an energy-dependent longitudinal delay of the electrons: the unmodulated particles are bent into a longer trajectory than the higher energy particles so that the beam is redistributed longitudinally. The process is referred to as "(micro)bunching". The modulator is tunable

in such a way that the created bunching gives maximum light output for either the resonant frequency of the modulator or a higher harmonic (Harmonic Generation). In the MAX-lab FEL project, the third harmonic will be used, thus efficiently shortening the output wavelength to 88 nm. In the second undulator, called radiator, the bunched beam will then emit intense, coherent radiation at the shorter wavelength with an output power in the megawatt-range. The 6 dimensional phase space file from ELEGANT is converted into a GENESIS input file by cutting out the seeded part of the beam and splitting it up into a collection of temporal slices. For each slice, the relevant beam parameters such as the average current, emittance, centroid and beam size are calculated externally and delivered to a GENESIS compatible input file.

FEL Simulation

The FEL consists of two different undulators as detailed in section . Table 3 lists the properties of both undulators and the intermediate magnetic chicane. The undulator parameter K was adjusted to yield optimal energy-modulation in the modulator and a high output power in the radiator. Time-dependent GENESIS simulations were performed to estimate the FEL output properties. At 88 nm, the temporal and spectral distribution of radiation power at the end of the radiator evolve as shown in figure 8. The corresponding output for the fifth harmonic, 54 nm can be seen in figure 9. In fact, it becomes clear that at 88 nm, the high current part of the beam lases with less intensity than the part with a low energy-spread. This shows the relevance of the beam energy-spread, as it counteracts micro bunching in the magnetic chicane. At 55 nm however, all beam slices appear to lase equally well independent of their energy-distribution, such that the temporal power profile closely resembles the current profile.

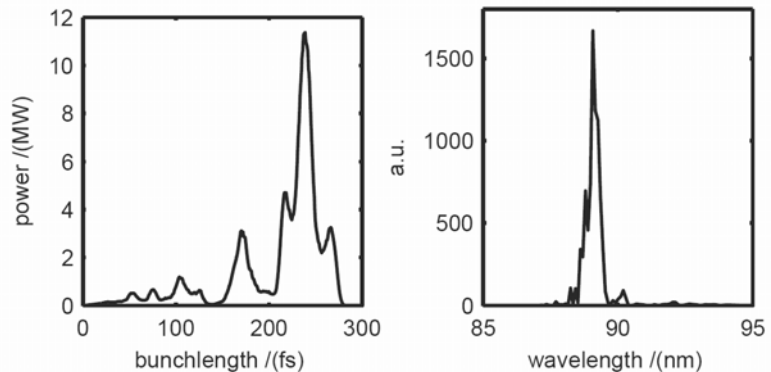


Fig. 8. Distribution of power along the bunch, and spectral power distribution, at the end of the radiator tuned to the 3rd harmonic.

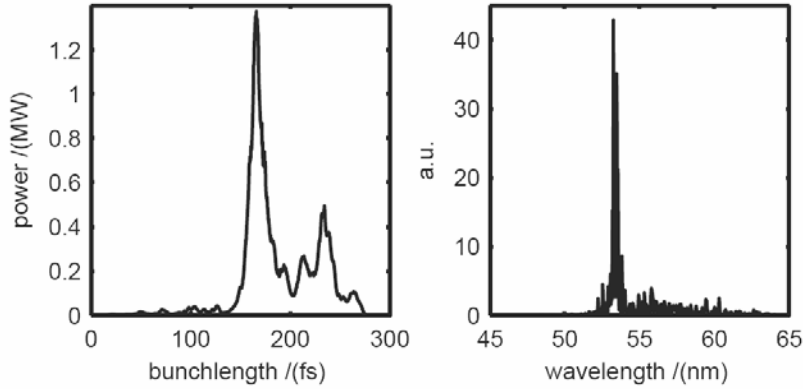


Fig. 9. Distribution of power along the bunch, and spectral power distribution, at the end of the radiator tuned to the 5th harmonic.

CONCLUSION

The FEL test facility at MAX-lab aims at reaching an output wavelength of 88nm with a seeded HG FEL. Start to end tracking simulations show that the generation, compression and transport of the beam from the existing MAX-lab injector to the FEL undulators can be done with a good electron beam quality maintained. In fully time-dependent FEL simulations, stable radiation at 88nm could be shown. Even lasing at the fifth harmonic at 54 nm could be seen. The results from the beam dynamic calculations give a short spike of electrons with high current which lead to a laser pulse of 30 fs duration and output power of 11 MW for 88 nm and 1.4 MW for 54 nm. Even higher laser power could have been achieved with a lower energy spread in the electron after compression. To accomplish this the existing facility at MAX-lab would have to be rebuilt so that the bunches are compressed before the final acceleration. Effects of wake fields was not calculated outside the accelerating structure and these might have a smoothing effect on the electron bunch. The overall result remains to be verified in experiments.

3 Gun systems

3.1 Gun 1

The initial electron source for the test FEL is a RF-gun with a BaO cathode [11]. This system is normally operated in thermionic mode for storage ring injection. The emission is strongly space charge limited and thus the emittance is not adequate for Harmonic Generation purposes. To reach an emittance of 3 mm mRad it is thus necessary to reduce the emitted charge to < 0.1 nC. The gun is also emitting a long pulse train not optimised for the synchronisation to the seed laser system.

The start up of the FEL test facility will be done by improving the emission process in the RF-gun by using a 10 ps laser pulse. The heating of the cathode can be reduced significantly below thermal emission and then gated by the seed laser. In thermionic mode the emission starts immediately when the accelerating fields pass the 0 phase. These first electrons carry a low energy and electrons emitted later will catch-up with the first ones creating a strong bunching on the ps scale. As the

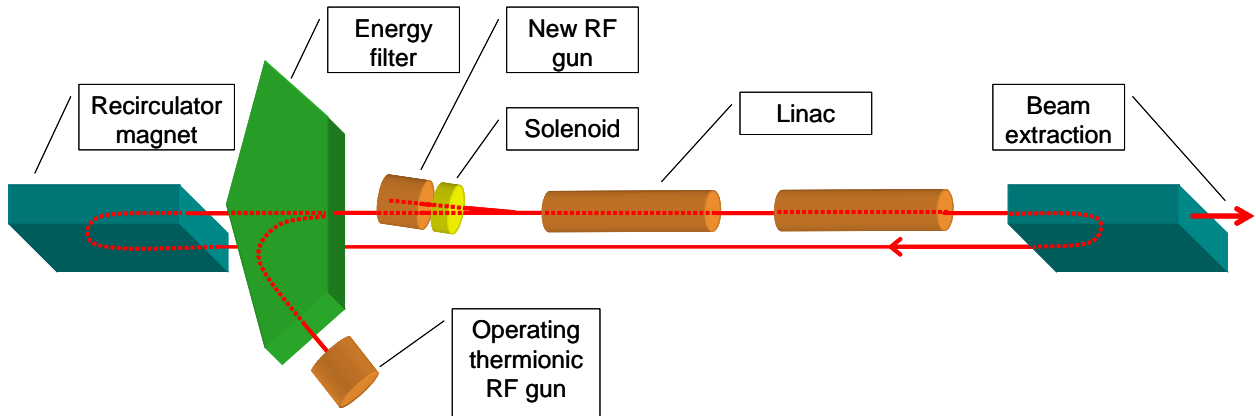


Fig 11. Schematic layout of the MAX injector

energies are low (a few 100 kV) the space charge effects are very strong disrupting the bunch both

transversally and longitudinally. A method to overcome this is to gate the emission process later in the RF phase (20-30 deg). Thus the initial bunching will be reduced. A 10 ps laser pulse at an RF phase of 30 degrees will result in a 7-8 ps long electron pulse. The charge density is reduced and the acceleration quicker and thus a reduced emittance is achieved.

The RF-gun in use at MAX-lab, though, is not completely optimised for ultra low emittance operation and thus the accelerated charge has to be limited to around 0.1 nC to achieve a normalised emittance in the range of 3 mm mRad according to simulations.

The gun laser and RF-gun have been operated together and full control of the synchronisation and emission phase have been achieved. The charge and emittance have not been measured at the moment. The charge has not been available due to the short pulse structure (< 10 ps) and the emittance has not been achieved due to a shortage of beam time.

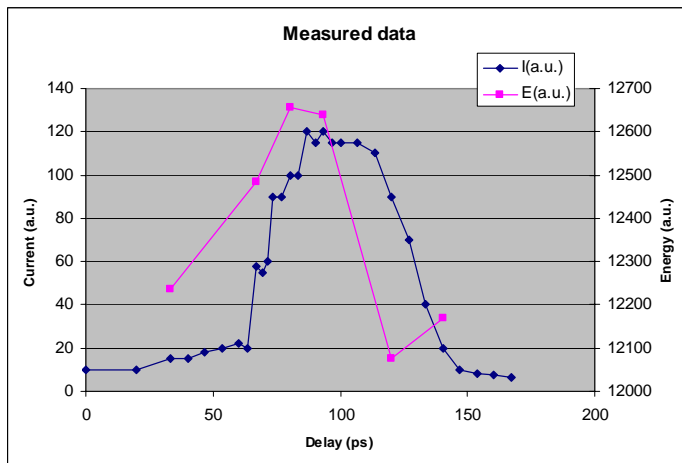


Fig 10. Measurements on the photoemission from the RF-gun system. Current (blue) and Energy (purple) as a function of the delay of the laser pulse. ($1 \text{ ps} \cong 1 \text{ degree phase angle}$)

The phase of the gun laser pulse relative the RF phase has been scanned and the relative current and energy has been measured (fig 10). The total emission phase is 60 degrees which is good agreement to simulations. The rise time of the emission while scanning the laser pulse over the 0-degree phase is slightly longer than expected. The Gaussian profile of the laser pulse can explain the main contribution but other effects are also relevant: acceptance of the beam transport to the current transformer, response of the current transformer etc. which has to be investigated. The energy of the extracted electrons follows roughly the expected performance, where optimal operation

phase is close to where the energy starts to drop (90 ps in fig 10.).

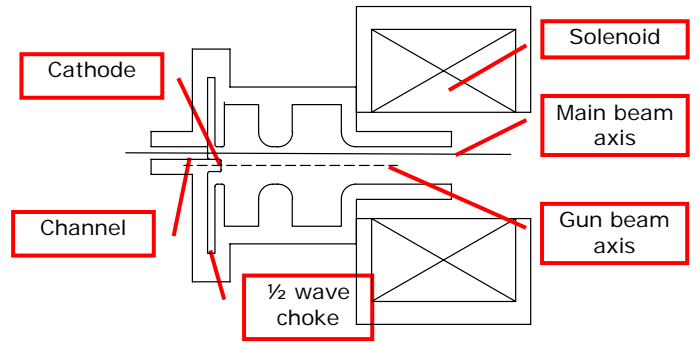


Fig 12. Drawing of the gun and compact solenoid assembly.

3.2 Gun 2

To improve the emission and to reach the specified emittance of 3 mm mRad while maintaining or increasing the bunch charge, a new gun structure is needed. Such a design is restricted by the existing injector which is a recirculated linac (fig 11). The solution adopted in the new design is a 3 GHz RF gun with an emittance compensating solenoid. A 10 ps laser system synchronised to the linac RF (and the seed laser for the FEL) will generate the electrons. The bunch will be compressed in the passage of the recirculation system [2] from 10 ps to the fs range.

The main design constraint turned out to be to allow for the recirculated beam in the system. As the beam passes twice through the linacs it is not possible to place the electron gun on axis. Further the available space is tightly restricted both in the longitudinal direction and by the beam axis being very close to the ceiling.

The gun geometry

The gun (fig 12) is based on the LCLS gun [12] adapted to European 3 GHz and changed to allow a beam channel close to the cathode. To minimize the influences by this additional channel close to the high field region a $\frac{1}{2}$ wavelength choke has been introduced. This choke is circular symmetric. The main 2D-design of the gun has been done in SUPERFISH [13] and limited resolution 3D-calculations have been performed in MULTIPHYSICS. Out of experience [11] SUPERFISH calculations are very accurate. As the final gun is not fully axial symmetric due to the waveguide coupling hole, the pumping hole and the recirculated beam channel 3D calculations were necessary (fig 13a&b). These do not fully agree with the 2D calculations, mainly due to limited computer power, but are accurate enough to study non axial symmetry deviations.

Table 3: Gun specifications (SUPERFISH, without waveguides and beam channel)

Q value	13900
Shunt impedance =	44 MOhm/m
Energy	3.7 MeV (kinetic)
Power consumption	3.9 MW
Max field strength on surface	121 MV/m

The recirculated beam channel does not influence the fields in the gun $\frac{1}{2}$ -cell significantly. The choke entrance close to the cathode surface gives an increased surface field strength though, and will most likely be the limiting factor for the excitation of the structure.

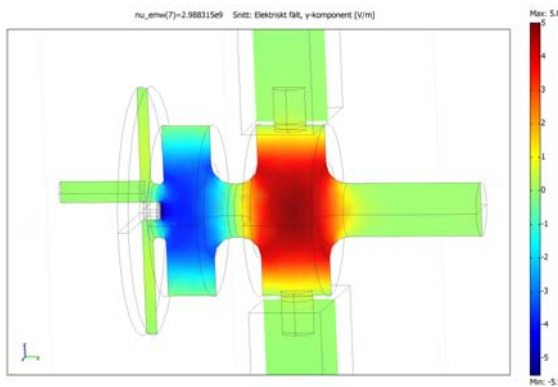


Figure 13a: Distribution of E-field component along the gun axis.

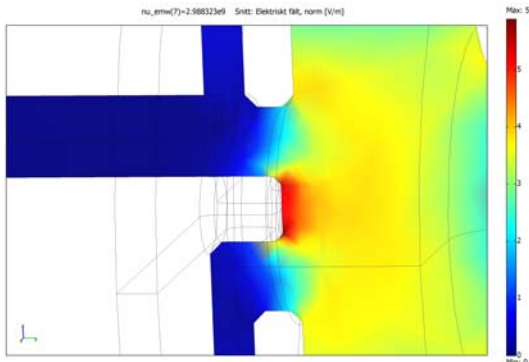


Figure 13b: Total field distribution at the cathode, choke entrance and additional beam channel.

The structure has a sensitivity for frequency which will be adjusted by a couple of thin wall positions which can be deformed and by a change in water temperature. This is not assumed to be a large problem. More problematic is the field balance between the $\frac{1}{2}$ -cell and the main cell. This balance can be changed by the deformable walls a/o changes in the depth of the choke (before brazing).

Optics

The emittance compensation scheme adopted is similar to the LCLS [12]. Due to space limitations the solenoid compensation magnet will be very compact.

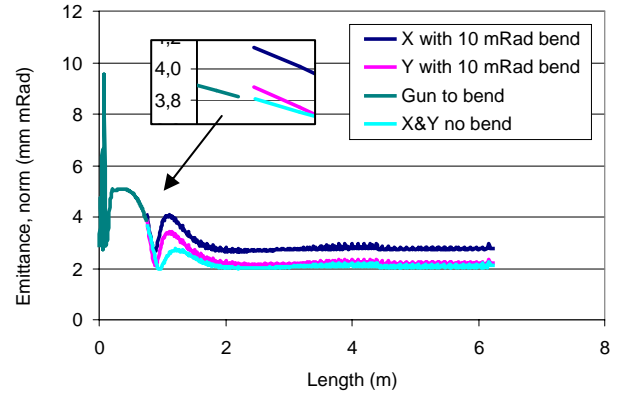


Fig 14. Emittance (normalised) (1 nC, 3.7 MeV, 10ps). Bending magnet (10mR) at 0.75 m and linac from 1m.

The beam from the electron gun is bent 10 mRad to get on the linac axis. This will increase the horizontal emittance slightly. Not only a direct increase in emittance is seen but the emittance compensation is also disturbed. Thus a final horizontal emittance increase of almost 50% is observed.

Simulation of the effect can not be done in ASTRA [5] as it does not treat bending elements. Thus the simulation is interrupted and swapped to *elegant* [6] and then moved back to ASTRA. By running *elegant* with only a drift section one can see that the program swap and lack of space charge effects in *elegant* are negligible at this location. Results of the tracking are shown in fig 14 and 15.

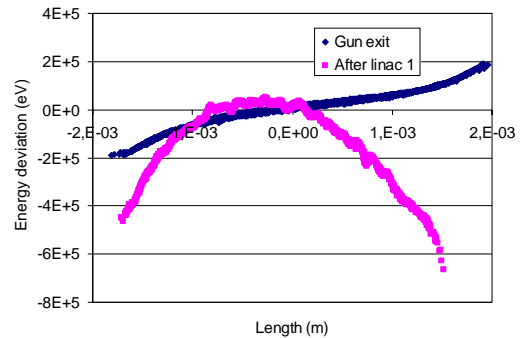


Fig 15. Energy distribution along the bunch (1 nC, 10ps) at the gun exit (4.2 MeV, total) and after linac 1 (108 MeV, total).

Solenoid and emittance compensation

To fit an emittance compensating solenoid (fig 12&16) onto the MAX injector a very compact magnet is necessary as the beam position is close to the ceiling. By allowing 70 mm flanges on the gun

the solenoid aperture can be kept fairly small. The wiring of the solenoid needs to be water cooled. No bucking coil to remove stray fields at the cathode surface are foreseen. The emittance increase due to such fields is negligible according to ASTRA simulations.

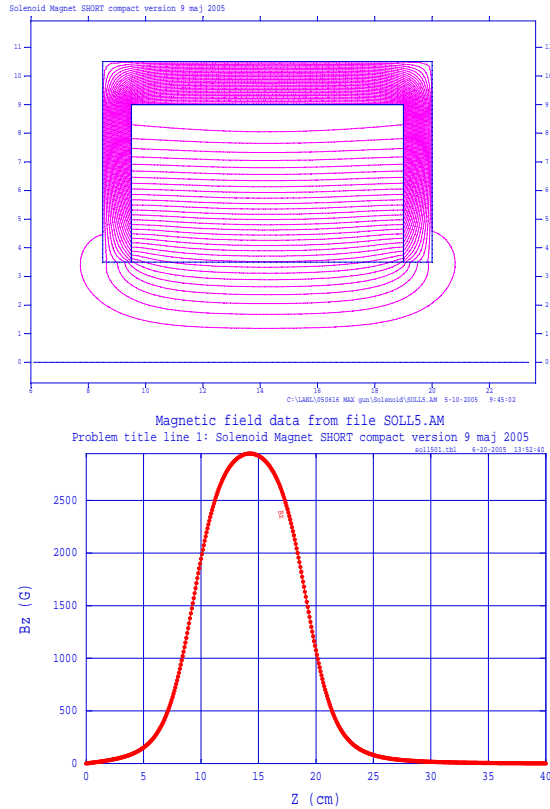


Fig 16. Solenoid geometry and field distribution

Summary

This gun design fulfils the goals on emittance and charge. The problems of space and recirculated beam are solvable, though an effect of the

performance can be seen. The gun structure is sensitive especially in field balance between the two cells and only the final brazed gun will show if the desired values can be reached. Further rather high field levels will be present and also here only the final fully conditioned structure will show if these levels can be reached.

A prototype of the gun structure has been machined and power RF tests performed. The recirculator is being rebuilt to give space for the new gun and the waveguide system to allow additional structures receiving higher powers.

3.3 Laser systems

The laser system is one combined system for both the electron gun and the seeding purchased as one unit, but placed separately in two laser hutches (fig 17 & 18). The two systems share one common oscillator locked to the 3 GHz RF system and are synchronised to each other by a fibre optical link.

The systems are installed and operated up to specifications. The spectral output from the two systems are given in fig 19 a and b and the pulse width of the gun laser, measured by autocorrelation, in fig 20. The results are summarised in table 4.

Table 4. Basic parameters of the laser system.

	Design requirements	Achieved
Gun laser	265 nm	263 nm
	500 μ J	550 μ J
	10 ps	10 ps
Seed laser	266 nm	263 nm
	100 μ J	140 μ J
	< 500 fs	350 fs

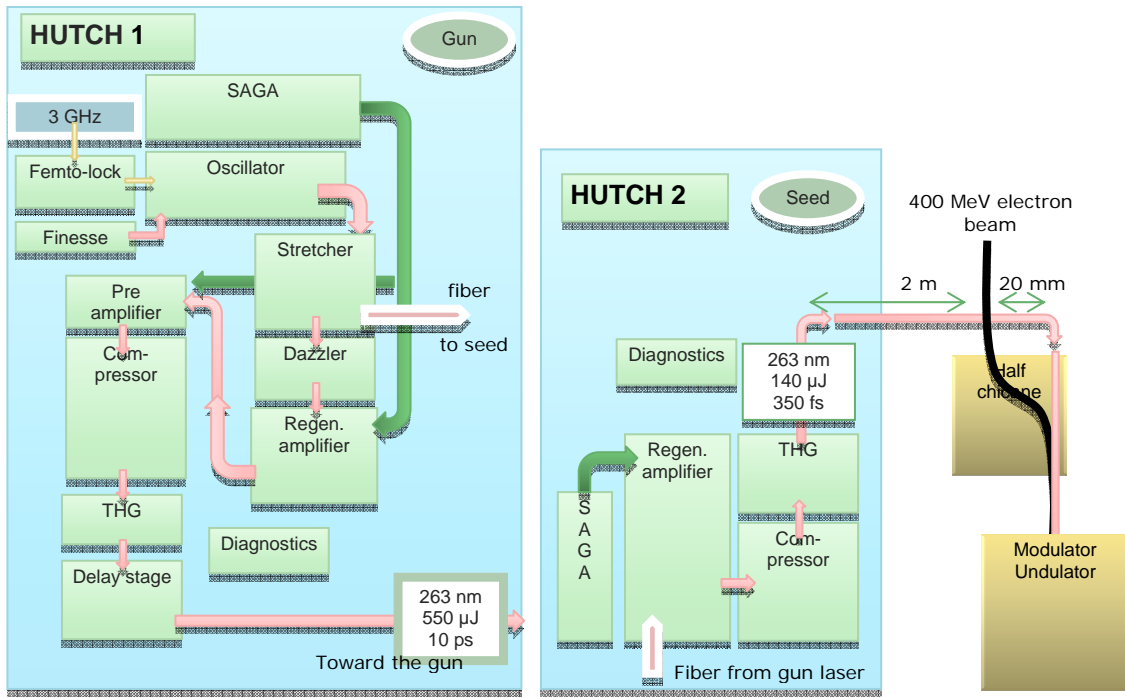


Fig 17. Layout of the gun and seed laser system.

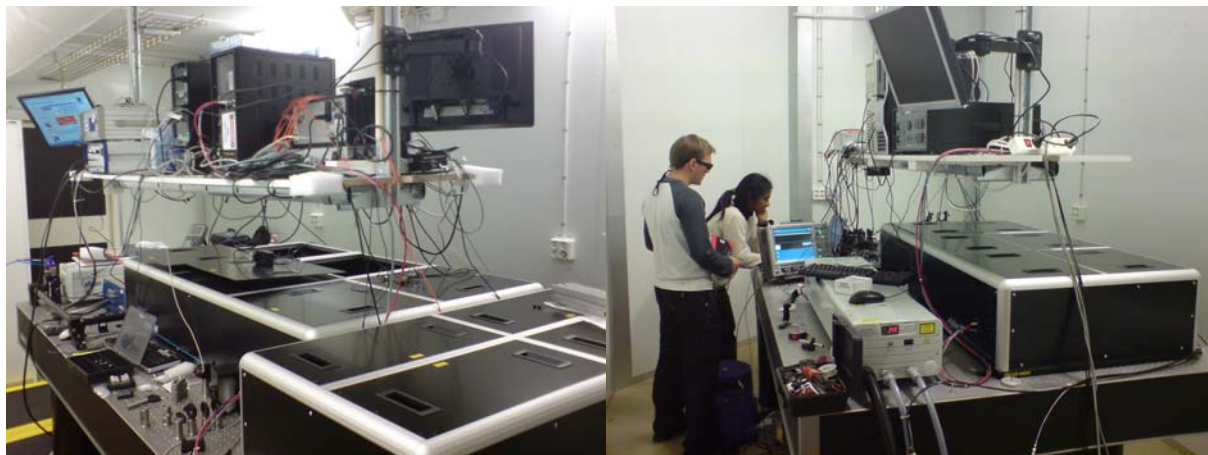


Fig 18. The gun laser system (left) and the seed laser (right) installed at MAX-lab.

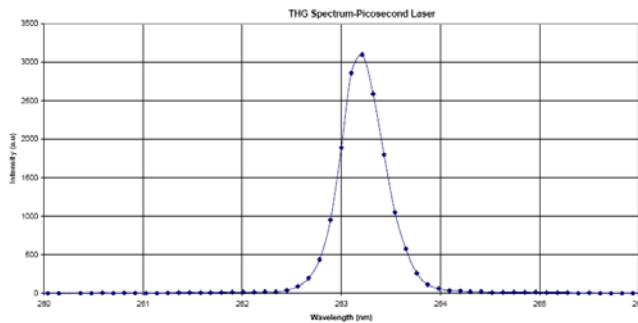


Fig 19a. Measured spectrum of the third harmonic in the output from the gun laser system.

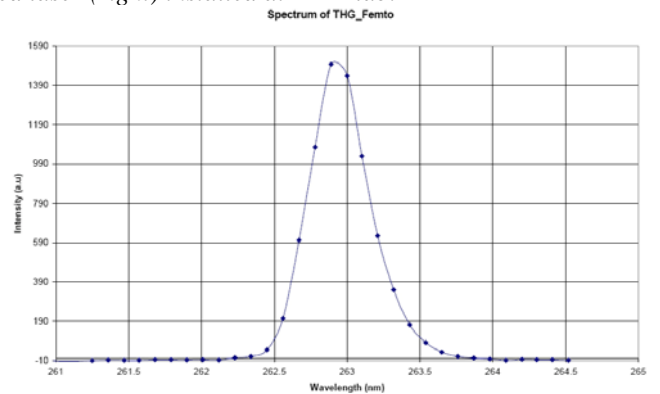


Fig 19b. Measured spectrum of the third harmonic in the output from the seed laser system.

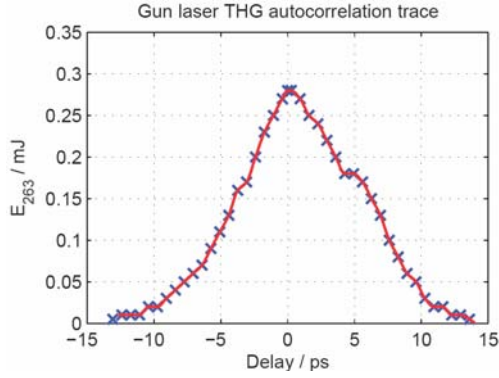


Fig 20. Autocorrelation measurement of the gun laser pulse. Assuming a Gaussian pulse gives a pulse width of 9 ps (FWHM).

4 Optical klystron

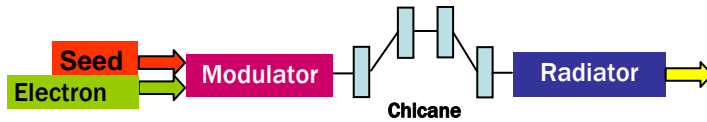


Fig 21. Principle layout of the seeded HGHG-FEL.

4.1 The undulators

Existing magnet structures were used to build the undulators. A pure permanent magnet (PPM) structure has been loaned from the ESRF to be used in the modulator. The radiator has been equipped with the APPLE structure of the BESSY UE56-1 [17]. The parameters are summarized in table 5. Figure 22 shows the achievable K-parameters for various undulator designs. The PPM curve refers to a gap of 10mm whereas the APPLE II curves have been evaluated for 12mm gap. The larger nominal gap of the radiator provides space for pure permanent magnet shims to compensate for the magnet block inhomogeneities [14].

Table 5: Parameters of the undulators and the chicane

Modulator	
Period length	48 mm
Number of periods	30
Minimum gap	10 mm
Maximum K-parameter	4.3
Radiator	
Period length	56 mm
Number of periods	30
Minimum gap	12 mm
Maximum K-parameter	4.3
Chicane	

Number of magnets	4
Type of magnet	H-frame, electromagnet
Gap	15 mm
Pole dimensions (length x width)	120 x 100 mm**2, including chamfer
Maximum current	3A
Maximum field	0.2 T
Distance between magnets	400 mm

At an electron energy of 500MeV the modulator (period length = 48mm), operating at smallest gap, is resonant to the seeding radiation of the laser. As the target energy is 450MeV a sufficient safety margin in the undulator design is provided. The radiator reaches the 267nm even in the vertical linear mode. The radiator will be operated at this wavelength for tests related to the possible application of optical replica synthesis [15]. The project goal is the production of 88nm (3rd harmonic of the modulator). The production of even shorter wavelengths will also be studied.

Both undulators will have a motorized gap drive. The radiator provides also a motorized phase variation for polarization control.

The modulator is moved only in case of an electron energy change whereas the radiator has to be tuned also when the harmonic number of the radiation or the state of polarization is changed.

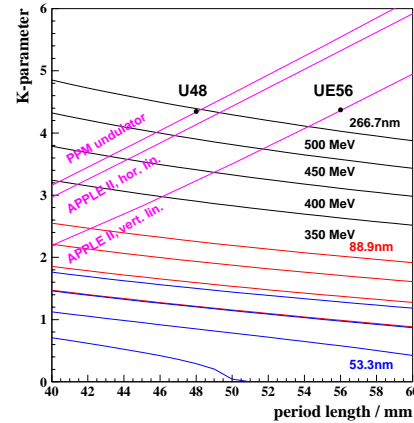


Fig 22. K-parameters for various undulator designs compared to K-parameters needed to generate 266.7 nm, 88.9nm and 53.3nm radiation for electron energies between 350-500MeV.

4.2 The chicane

The magnetic chicane converts the energy modulation of the electron beam into a spatial modulation. Optimum bunching is achieved if the energy modulation dominates the energy spread times the harmonic number n :

$$\Delta\gamma / \gamma \geq n \cdot \sigma_\gamma$$

With a relative energy spread of $\sigma_\gamma = 5 \cdot 10^{-4}$ an energy modulation of at least $\Delta\gamma/\gamma = 1.5(2.5) \cdot 10^{-3}$ is needed to operate on the third (fifth) harmonic. This defines the laser power.

The maximum bunching appears for a path length difference of $\Delta L = \lambda_{\text{photon}}/4$ between modulated and non modulated electrons. The chicane is optimized such that $\Delta L = \lambda_{\text{photon}}^{1st}/4 = 67\text{nm}$ can be reached with 500MeV electrons and an energy modulation of $\Delta\gamma/\gamma = 1.0 \cdot 10^{-3}$. For higher harmonics (shorter wavelengths) $\Delta L \geq \lambda_{\text{photon}}/2$ can be produced and overbunching effects can be studied.

The distance between the magnet centres is 400mm. This provides sufficient space for the installation of diagnostics.

In principle, the chicane can be realized either as a permanent magnet device or as an electromagnet. Both designs provide a tuneable delay. An electromagnetic design has been chosen due to the better field homogeneity (figure 23). Additionally, it can completely be switched off, which is of advantage when commissioning the undulator sections with beam.

The chicane consists of four electromagnets (Fig. 24). Each magnet is made of two low carbon steel pieces ($C < 0.01\%$) which are bolted together. The poles have been wire cut. The number of windings per coil is 432. The measured field integrals per Ampere for the four magnets are: 10.9, 10.9, 10.6, 10.7 Tmm / A. The magnetic hysteresis of the four magnets as measured with a moving wire is ± 0.25 Tmm (Fig. 25). Hall probe measurements show a reproducibility of the field setting below $5e-4$ after two cycles (Fig. 25).

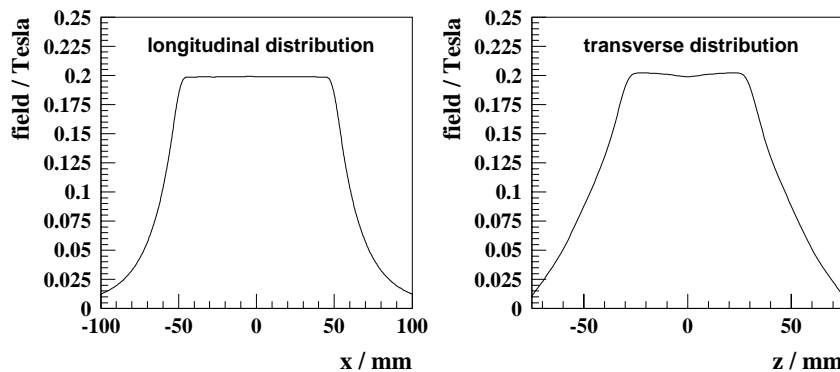


Fig 23. Longitudinal and transverse field distribution of one chicane magnet.



Fig 24. Electromagnetic Chicane.

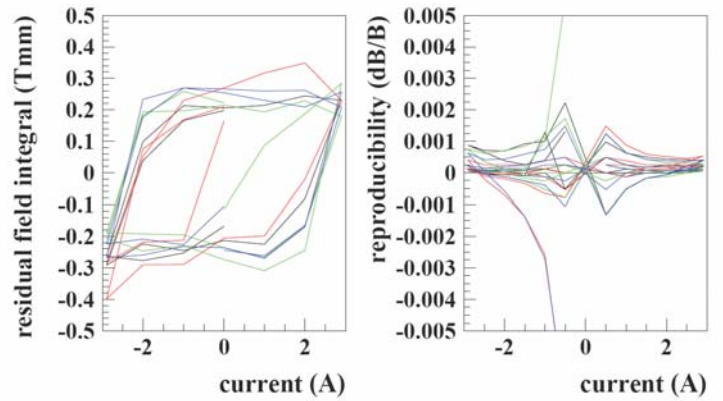


Fig 25. Left: Hysteresis of field integrals of the four magnets. The measurement noise is due to the presence of up to 30Tmm field integrals. Right: Reproducibility of field settings within a sequence of several current cycles of the magnets.

4.3 Mechanical Layout

The electron beam height at the HGHG-FEL is only 520 mm and conventional undulator carriages cannot be used here. Elevating the beam height to 1.2m would require additional magnets and space and the beam quality, especially the beam emittance, would suffer from this extra deflections.

Therefore, a new carriage has been developed which can cope with this geometry (figure 26). The same structure is used for both undulators. The accuracy is achieved with a stiff welded structure. Four sleds are driven with right and left threaded ball screws. The modulator is driven with one servo motor. The optional tapering requires two motors for the radiator. The gap

encoder is located in a line with the electron beam to avoid Abbe's comparator error [16].

The undulators have been measured and shimmed at the existing measurement bench at BESSY. For this purpose the undulators have been flipped into the upright orientation (figure 27). At MAX-lab the final measurements have been performed in the operating position using a pulsed wire system. Air coils at either end of each undulator are used to compensate residual field integrals.

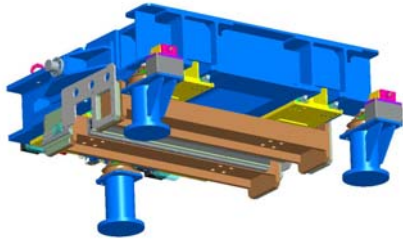


Fig 26. Modulator in operating position.

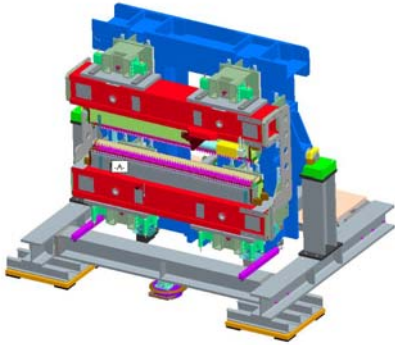


Fig 5. Radiator in measurement position.



Fig 28. Radiator of the APPLE II type in operating position without vacuum chamber. Four power meter sensors (see below) at each undulator end (orange cable) are installed.

5 THZ DIAGNOSTICS

The diagnostics of the FEL resonance in the modulator will be performed using a strong

difference in coherent THz emission [18, 19] from the seeded and unseeded bunch after propagating through an additional bending magnet (dump magnet) behind the radiator. Since the electrons are gathering path length differences controlled by R56 along the magnet, the bunch shape in time domain is different for the seeded and unseeded case. This is caused by the change in energy spread due to the FEL resonance (Fig. 29 left).

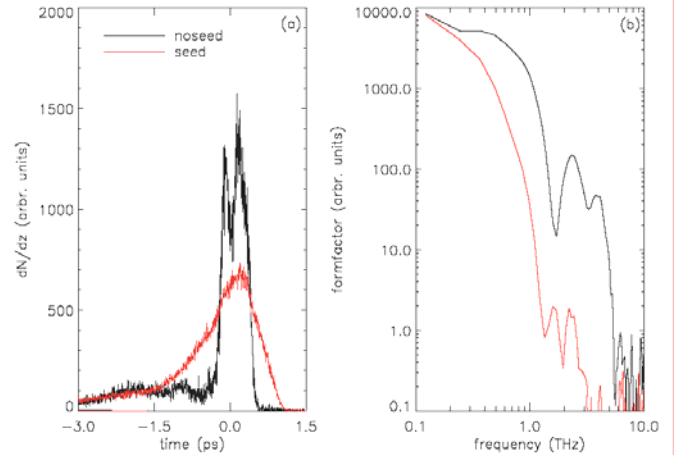


Fig 29. Left: Projection of the seeded and unseeded electron density in the bunch according to start-to-end simulations [20] after passing an R56 of 0.05 m. Right: Expected envelopes of THz spectra (formfactor) emitted by these bunches for the seeded and unseeded case.

The THz power spectral density emitted there is $\sim N(N+1)f$, where f is the square of the Fourier transformation of the longitudinal electron density and $N=0.6 \times 10^9$ (0.1 nC) is the number of electrons. The calculated form factor f for the two cases (Fig. 29, right) demonstrates that the coherent far infrared emission in the range between 1 and 10 THz can be employed to detect the overlap between seed laser and bunch in the modulator. By setting an appropriate high pass filter the signal from a THz detector will almost completely drop to zero for a successful energy modulation of the electrons.

6 Radiation measurement systems

RADIATION PROTECTION OF THE MAGNETS

Significant demagnetization of undulator permanent magnets in storage rings have been reported in the literature [21, 22]. The risk of demagnetization is even higher in single pass devices like linac based FELs. Extensive studies have been performed to get a quantitative understanding of demagnetization effects [15, 16]. Collimation systems have to be designed such that the radiation dose deposited into the magnets remains below an acceptable limit [23].

In the MAX-lab FEL a stainless steel capillary (length: 100mm, diameter 3mm, wall thickness:12.5mm) is located in front of the modulator preventing the electron beam from hitting the circular beam pipe in case of a failure of the two vertical deflecting dipole magnets at the laser beam port (vertical beam displacement due to the dipole magnets: 20mm). The electron losses will be monitored with two different systems, a Cherenkov system for fast beam loss detection and a powermeter system for absolute dose measurements. GEANT simulations have been performed to estimate the radiation doses in the magnets and to evaluate the corresponding number of produced Cherenkov photons. The experiences gained with these systems will be valuable for the BESSY Soft X-Ray FEL [24].

Cherenkov System

A Cherenkov fiber system [25] is fast and the signal can be used to switch off the electron beam in case of intolerable beam losses. During the commissioning phase the relative intensities of the individual fibers can be used to align the electron beam properly. The system installed at the MAX-lab FEL consists of four radiation insensitive glass fibers (core: 300 μm , cladding: 300 μm) mounted directly onto the circular undulator vacuum chamber which has a diameter of 10mm (Fig. 30). Thus, the fibers will provide detailed spatial information even for large undulator gaps. The sensitivity of the fibers is small as compared to large luminescence detectors. The small size, however, permits an installation close to the electron beam over many meters. The GEANT [28] simulations are based on a 1nC bunch hitting the vacuum chamber wall of the modulator under zenith angles of 0.1 and 1mrad and azimuthal angles of 0, 45 and 90 $^\circ$, respectively. Four Cherenkov fibers and one Thermo Luminescence Detector (TLD) are included in the model (Fig. 30). The evaluated radiation doses induced in the TLD and the magnets and the produced Cherenkov photons are summarized in (Tab. 6). The given number of photons is the number detected by the photomultiplier (applying a numerical aperture of 0.22 inside the fiber and including the spectral characteristics of the multiplier).

Maximum doses of 0.59 Gy/nC are detected for the 1mrad case (Fig. 31). It has been shown [26] that a maximum reduced dose (electron energy > 20MeV) of 70kGy can be tolerated in case of the BESSY Soft XRay FEL which represents a rather conservative number for the short MAX-lab FEL. Thus, the number of generated Cherenkov photons is sufficiently high to detect even small electron

beam losses long before the magnets are damaged. The exact detection limit of the Cherenkov fibers will be subject to further studies.

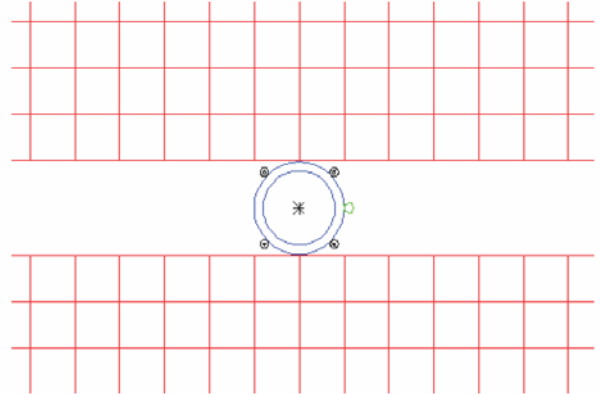


Fig 30. Cross section of the modulator including the permanent magnets (red), vacuum chamber (blue), Cherenkov monitors (black) and TLD monitor (green).

Table 6. Results from GEANT simulations.

angles mrad / $^\circ$	TLD mGy / nC	max. dose in magnet mGy / nC	Cherenkov photons/nC	
			forward direction	backward direction
0.1 / 0	1207	57	6.7e7	1.1e7
0.1 / 45	131	205	9.7e7	1.5e7
0.1 / 90	77	287	7.2e7	1.2e7
1.0 / 0	2730	188	1.2e8	2.1e7
1.0 / 45	412	487	1.6e8	2.7e7
1.0 / 90	279	588	1.3e8	2.3e7

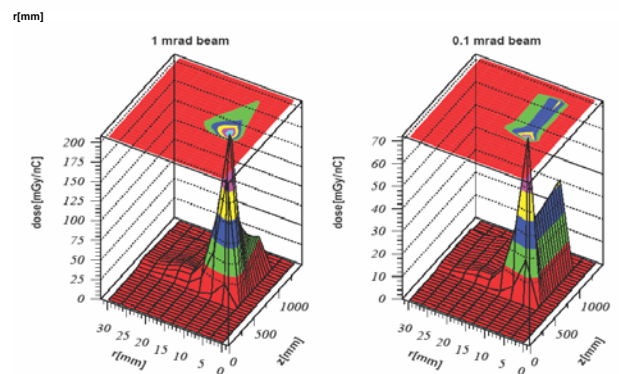


Fig 31. Radiation doses inside the magnets induced by a 1nC electron bunch hitting the vacuum chamber. The data are averaged over the 0 $^\circ$, 45 $^\circ$ and 90 $^\circ$ scenarios.

Powermeter System

Absolute radiation dose measurements can be done with calibrated glass fibers [27]. The fibers can be installed along the region of interest (e.g. the

complete undulator system) providing spatial information of the beam losses (Optical Time Domain Reflectometer, OTDR). Another approach is a system of several local sensors which are multiplexed. The spatial resolution of the latter system is slightly lower (depending on the number of channels) but the complete dynamic range is available for each channel whereas in the OTDR system the dynamic range is available only for the whole system. A system with 16 local sensors has been installed at the MAX-lab FEL. Glass fibers for telecommunication applications are not optimized for radiation dosimetry. Usually, the optical parameters which are relevant for dose measurements can vary by orders of magnitude. This requires a careful selection of the fibers. Four germanium and phosphorous doped polyimide coated 50/125/145 μm graded index fibers from different suppliers have been tested by the Fraunhofer INT, Euskirchen, Germany. A fiber fabricated by J-Fiber, Jena, Germany, has been selected for the MAX-lab FEL. The calibration of this fiber as determined with a Co-60 source is plotted in figure 32. The figure of merit for the fiber selection is a combination of various parameters: i) high dynamic range; ii) radiation sensitivity; iii) annealing after irradiation; iv) linear response on total radiation dose; v) low sensitivity on dose per time.

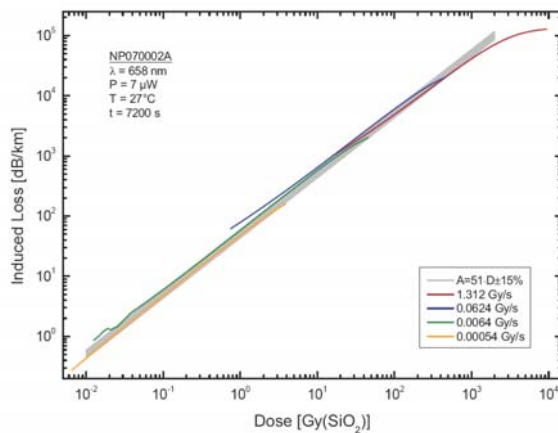


Fig 32. Calibration of the selected fiber.

The chosen fiber has the following performance (Fig. 32): i) in combination with the currently installed light source and the power meter the dynamic range is 30-40 dB ii) the attenuation is described by: $(\text{dB} / \text{km}) = \text{dose} (\text{Gy}) * 51$. For comparison: the sensitivity of conventional germanium doped 50/125/250 μm graded index fibers as used to connect the sensor modules to the light source and the analyzer is two orders of

magnitude lower. iii) 24h after irradiation less than 10%. iv) The deviation from a linear curve within the range from 0.01- 1000Gy is smaller than $\pm 15\%$. v) A linear response has been demonstrated for dose rates between 0.0005 Gy/s up to 1.3 Gy/s. The MAX-lab system consists of sixteen channels. One channel serves as a reference. The read out time for all 16 channels is less than 60s. The light source consists of an LED (658 nm) powered by a stable constant current power supply. 10% of the output power is measured directly (excluding the optical coupler, the optical switches and all fibers) with a power meter. In a temperature stabilized environment the source drifts are only 0.01dB / day. The influence of typical source drifts in a rough environment of 0.02-0.05dB / day can easily be compensated. The reference fiber has no sensor module attached but is shortcut at the FEL location. It can be used to compensate for drifts of the support fibers. The sensor fibers are wound to rectangular flat coils (50x50mm**2) and the radiation exposed length of one fiber is approximately 2m. The coils are mounted onto the magnet girders close to the upstream and downstream ends of the undulators. At smallest gap the distance to the electron beam is 7mm for the modulator and 28mm for the radiator. Radiation sensitive fibers are used only for the coils. The distance of 40m between the FEL and the electrical cabinet is bridged with radiation insensitive fibers. The system has been installed in March 2007 and the drifts have been monitored since that time. The optical transparency of the 15 fibers has been corrected for fluctuations of the light source. The signals show a long term drift of $\pm 0.03\text{dB}$ per day and a periodic structure superimposed to it (Fig.33, left). The drifts are dominated by temperature fluctuations which is concluded from a correlation diagram (Fig. 33, right). The various fibers show individual temperature dependencies. The data can numerical and experimental studies at the FEL. be corrected using a specific temperature coefficient for each fiber. Two temperature sensors are installed at each undulator end. After correction the residual drifts are well below $\pm 0.01\text{dB}$ for a period of several days. This guarantees a long term system sensitivity of better than 0.2Gy. The remaining differences between the fibers are due to the individual characteristics of the cascaded optical coupler behind the light source. In case the fibers have reached the upper limit of the linear regime of 1000Gy they can be thermally annealed at a temperature of up to 350°C in order to recover the full transmission.

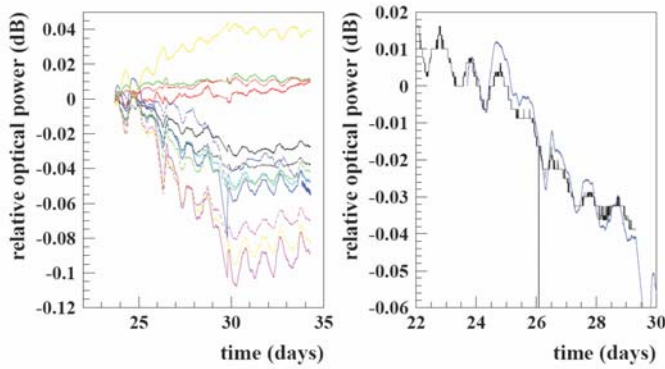


Fig 33. *Left: Long term stability of the system consisting of 15 fibers. Right: The day by day fluctuations (blue) are closely correlated to the temperature variations (black).*

7 First operations

Most of the experience gained with the system so far is qualitative, meaning that experience and the possibility of transporting the electron beam and laser beams has been approached. The first dedicated experimental period in December 2007 was used to such preparations. Two modes have been explored and the available results are given below.

Long pulse mode

The injector system at MAX-lab normally operates in a “long pulse” mode where the RF-gun cathode is used thermionically. This produces a 50 ns pulse train of around 15 pulses, each a few ps in length. This pulse is not suitable for generating harmonic photons at shorter wavelengths due to the poor emittance, but as it carries a larger total charge it is well suited for first operations of the beamline.

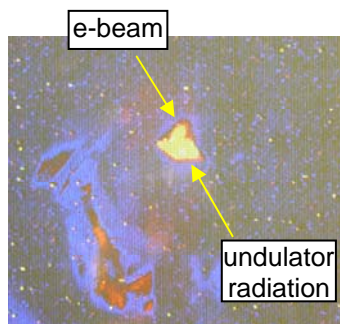


Fig 34. *Image of electron beam OTR and synchrotron radiation from the radiator undulator in long pulse mode. The OTR is generated on the mirror surface while the synchrotron radiation is reflected on the surface giving rise to the separation.*

The long pulse has been transported through the optical klystron of the system with the correct beam position. The functionality of the “half chicane” allowing seed laser injection has been verified. The chicane for microbunching has been operated and the field balance checked. The two undulators (modulator and radiator) have been operated and spontaneous synchrotron radiation produced (fig 34). The operation of all these system has thus been verified.

Short pulse mode

In short pulse mode the RF-gun is used as a photo cathode gun. The temperature of the cathode is reduced to below thermal emission and electrons generated by the 10 ps gun laser system. It is also possible to maintain a weak thermal emission to simplify the timing of the system during commissioning. The gun laser system has been synchronised to the 3 GHz RF system of the gun and linacs (fig 36). Electrons have been generated and transported through the linac system reaching 400 MeV. The final part of the transport still remains to be passed, before reaching the optical klystron.

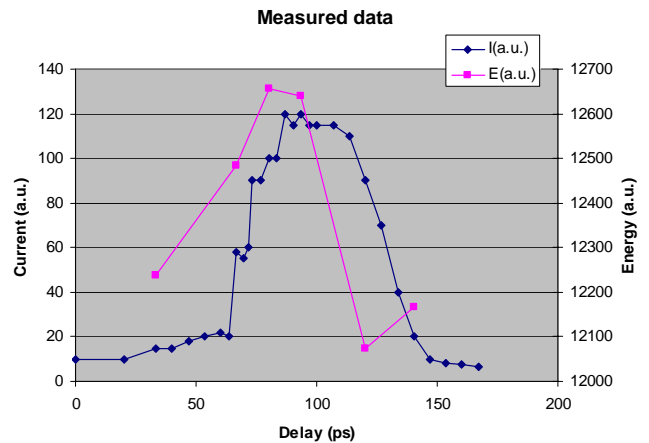


Fig 35. *Measured current and electron energy as a function of relative phase of the laser pulse on the cathode.*

Control of the timing (phase) between the gun laser pulse and the 3 GHz RF system has been achieved. The phase of the gun laser pulse has been scanned over the 3GHz cycle (fig 35) and the electron beam current and energy measured. The rising edge of the extracted current (fig 35) should reflect the gun laser pulse length of 10 ps but still show a slightly longer pulse. The optimal phase is, according to simulations, around 30 deg (~30 ps) when the electron energy starts to drop. This point is clearly identified and reproducible.

The radiation measurement systems have been tested during operation. The power meter system clearly shows the radiation deposited in the two undulators (fig 37). The top curve shows how the beam is reaching further and further into the first undulator. The bottom curve shows the readings in the second undulator. There is little signal until the first undulator is passed. Also the recovery of the fibres after the operation stops can be seen.

The Cherenkov system installed along the vacuum chambers resolves the longitudinal position along the undulators (fig 38). The main peak is from the first undulator and the second peak from the second undulator. Due to trigger problems the longitudinal resolution is not perfect. By tuning the system the “losses” can be moved to different positions along the beamline.

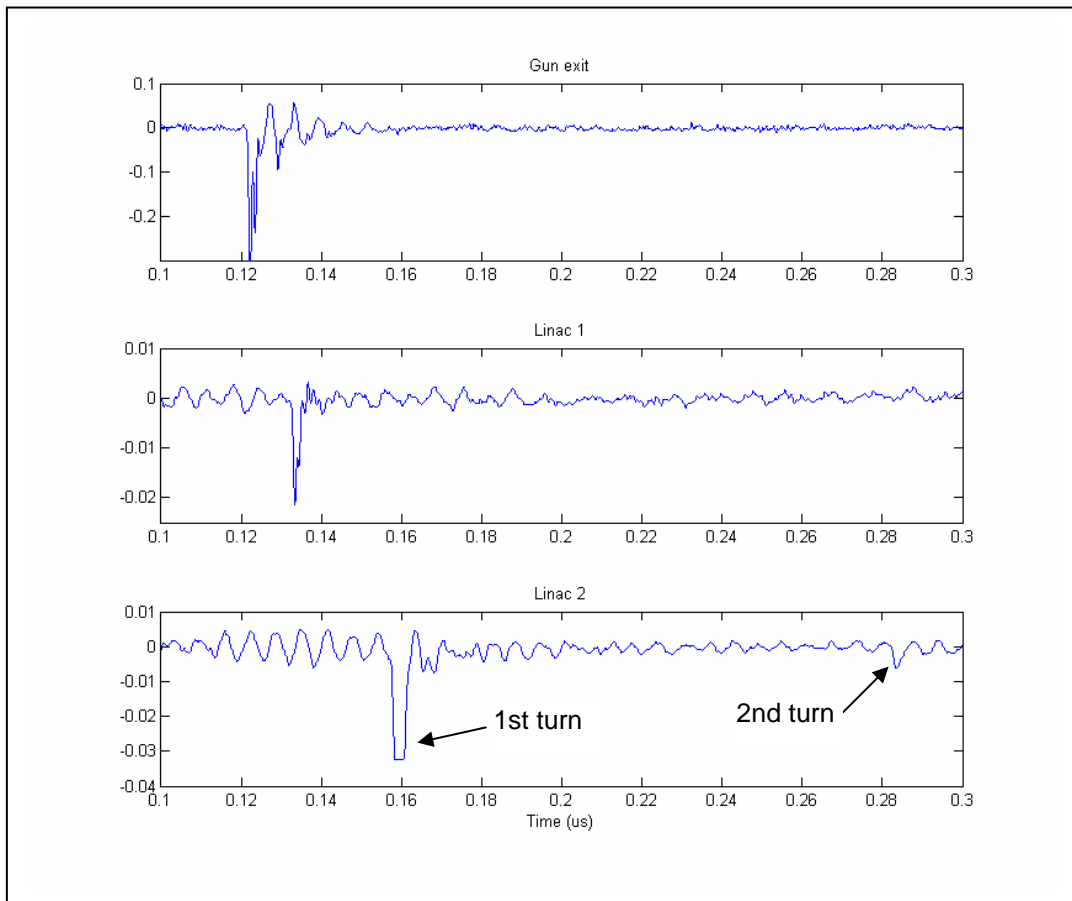


Fig 36. Electron pulses in short pulse mode (generated by the 10 ps gun laser). Current transformer pulses which do not resolve 10 ps. top: at gun exit, middle: at Linac 1, bottom: at After linac 2. First passage (200 MeV) is saturated, second passage (400 MeV) 120 ns later. (timing between signals is given by both different locations, and cable length differences.)



Fig 37. Power meter system readings during one of the first operation shifts.)

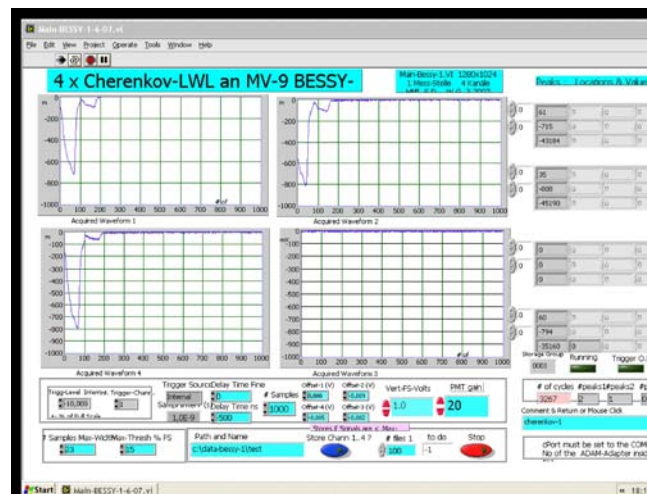


Fig 38. Output from the Cherenkov system in one of the first runs. One fibre is out of operation.

8 Summary

The complete set up for the test FEL has been built in the BESSY Max-lab collaboration. The subsystems have been designed, constructed built and installed on site. Simulations of the basic performance have been achieved and commissioning of the sub systems is complete. The work to put the whole system into operation has been started and the first results is starting to come.

The objectives of these activities within EUROFEL has been “to find answers and to test techniques essential for the design of the seeding and high-gain harmonic-generation (HGHG) mechanisms of the new VUV-X-ray FELs in Europe”. Several answers in the process of analysing and designing this kind of facility has been achieved. Also a number of techniques have been tested.

This work has been partially funded by the EU under the 6th Framework programme, contract no. 011935 EUROFEL.

References

- [1] L. H. Yu, J. Wu, Nucl. Instr. and Meth. in Nucl. Res. A 483 (2002) 493.
- [2] S. Werin et al., Commissioning of the 500 MeV Injector for MAX-lab, EPAC 2004
- [3] J. Bahrtdt et al., *Undulators for a Seeded HGHG-FEL at MAX-lab*, EPAC 2006.
- [4] M. Abo-Bakr et al., *Start to end simulations for the BESSY FEL project*, Nucl. Instr. and Meth. A 528 (2004) 476-480.
- [5] K. Flttman "ASTRA User Manual", September 18, 2000, www.desy.de/~mpyflo
- [6] M. Borland, "Elegant: A flexible SDDS-Compliant Code for Accelerator Simulation", APS LS-287, 2000.
- [7] V.K. Bharadwaj et al, *Linac Design for the LCLS Project at SLAC*, PAC97, 94309.
- [8] R.V.Servranckx, "User's Guide to the Program Dimad", TRIUMF Design Note, TRI-DN-93-K233, 1993
- [9] S. Reiche, "Numerical Studies for a Single Pass High Gain Free-Electron Laser", PhD Thesis, Uni Hamburg, corona.physics.ucla.edu/~reiche/links.html
- [10] C. Sung et al., *Seeded free-electron and inverse free-electron laser techniques for radiation amplification and electron microbunching in the terahertz range* Phys. Rev. ST Accel. Beams 9, 120703 (2006)
- [11] B. Anderberg, Å. Anderson, M. Demirkan, M. Eriksson, L. Malmgren and S. Werin, The design of a 3 GHz thermionic RF-gun and energy filter for MAX-lab, Nucl. Instr. And Meth. In Phys. Res. A 491 (2002) 307
- [12] R. Boyce, D.H. Dowell, J. Hodgson, J.F. Schmerge, N. Yu, Design Considerations for the LCLS RF Gun, LCLS TN 04-4 (2004)
- [13] K. Halbach and R. F. Holsinger, "SUPERFISH - A Computer Program for Evaluation of RF Cavities with Cylindrical Symmetry", Particle Accelerators 7 (1976) 213-222
- [14] J. Bahrtdt et al., Ninth International Conference on Synchr. Rad. Instr., Daegu, Korea, 2006.
- [15] E.L. Saldin et al., Proceedings of the 2004 FEL Conference, pp. 375-378.
- [16] J. Bahrtdt et al., Proceedings of the 2004 FEL conference, Trieste, Italy, pp 610-613.
- [17] J. Bahrtdt et al., Proceedings of the EPAC 2006, Edinburgh, Scotland, 2006, pp 59-61.
- [18] Holldack et al. PRL 96, 054801 (2006).
- [19] A. A. Zholents and K. Holldack, Proceedings FEL Conference 2006, Berlin, Germany, 2006, pp725-727.
- [20] S. Thorin, M. Brandin, S. Werin, K. Goldammer, and J. Bahrtdt , *Start-to-end simulations for a seeded harmonic generation free electron laser*, Phys. Rev. ST Accel. Beams 10, 110701 (2007)
- [21] P. Colomp, T. Oddolaye, P. Elleaume, "Partial Demagnetization of ID6 and Dose Measurements on Certain Ids", Machine Technical Note 1-1996/ID, 1996.
- [22] M. Petra et al., Nucl. Instr. and Meth. in Phys. Res. A, 507 (2003) pp. 422-425.
- [23] H. Schlarb, "Collimation System for the VUV Free- Electron-Laser at the TESLA Test Facility", Thesis Work, Universität Hamburg, DESY-THESIS-2001- 055, Nov. 2001.
- [24] "The BESSY Soft X-Ray FEL", Technical design Report, D. Kraemer et al., Berlin, 2004.
- [25] M. Körfer, W. Göttmann, F. Wulf, J. Kuhnenn, Proceedings of DIPAC 2005, Lyon, France, 2005, p301.
- [26] J. Bahrtdt et al., Proceedings of the FEL Conference 2006, Berlin, Germany, 2006, pp521-528.
- [27] H. Henschel, M. Körfer, J. Kuhnenn, U. Weinand, F. Wulf , Nucl. Instr. and Meth. in Phys. Res. A 526 (2004) pp. 537-550.
- [28] GEANT 3.21, Detector Description and Simulation Tool, Computing and Networks Division, CERN, Geneva, Switzerland.